

# MICROSTRUCTURAL CHARACTERIZATION OF SINGLE-CRYSTAL NICKEL-BASE SUPERALLOYS BY SMALL-ANGLE NEUTRON SCATTERING

Pavel Strunz<sup>1,2</sup>, Ralph Gilles<sup>3</sup>, Debashis Mukherji<sup>4</sup>, Albrecht Wiedenmann<sup>2</sup>, Rajeshwar P. Wahi<sup>2</sup> and Jozef Zrník<sup>5</sup>

<sup>1</sup>Nuclear Physics Institute, 25068 Řež near Prague, Czech Republic, e-mail: strunz@ujf.cas.cz

<sup>2</sup>Hahn-Meitner-Institut, Berlin, Germany

<sup>3</sup>University of Technology, Darmstadt, Petersenstr. 23, 64287 Darmstadt, Germany

<sup>4</sup>Technical University Braunschweig, Germany

<sup>5</sup>Technical University, Košice, Slovakia

## Abstract

The paper covers results achieved in investigation of precipitate microstructure of some nickel-base superalloys by means of small-angle neutron scattering using the V4 facility of BENSC, Hahn-Meitner-Institut (HMI) Berlin. Several interesting examples of recent investigations of SC16, SCA and ZS26 superalloys are reported. This overview also describes the outline of the SANS-data evaluation procedure.

## 1. Introduction

The two-phase microstructure consisting of  $\gamma'$  precipitates coherently embedded in the  $\gamma$ -phase matrix is the basic feature which determines the outstanding creep-resistance of nickel-base superalloys. These materials are frequently used for high-temperature applications, e.g. in aircraft turbines and in land-based gas turbine blades. After standard heat treatment of the original material, the precipitates are of cuboidal form and oriented with edges parallel to  $\langle 001 \rangle$  crystallographic directions. Moreover, they are often ordered into the three-dimensional grid (see Fig.1). Mechanical properties of these materials strongly depend on the morphology of the precipitates and thus also on the applied heat treatment.

The microstructure is conventionally studied by transmission electron microscopy (TEM), however, this and other standard methods of materials science do not usually characterize the microstructure completely. They provide usually only "local" information and it is frequently difficult to determine precisely the volume fraction. Small-angle neutron scattering (SANS), which yields bulk-averaged information on the parameters of microstructure (i.e. on precipitate shape, size, distance between precipitates as well as on volume fraction), has been found to be a powerful tool for investigation of microstructural inhomogeneities in single-crystal alloys [1-3]. In single crystal, SANS - due to the high penetrability of neutrons - can be used for investigation of different orientations (in certain angular range) of bulk material without need to prepare individual specimen for each orientation. SANS also allows to study early stages of precipitation in single-crystal alloys [1]. A number of studies (see e.g. [4-8]) documents an applicability of SANS particularly to investigation of precipitation in single-crystal Ni-base alloys. Moreover (as will be

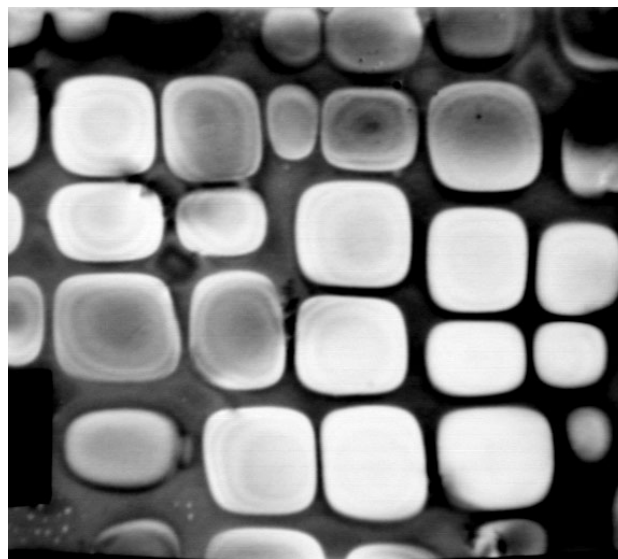


Fig. 1: An example of the cuboidal precipitate microstructure of Ni-base superalloy SC16 after standard heat treatment (TEM dark field image).

shown below when presenting investigation of SC16 superalloy) there are some kinds of precipitates for which small-angle neutron scattering is the only effective method for their characterization in the bulk material.

An overview of the recent studies of precipitate microstructure of ZS26 as well as of SC16 and SCA superalloys on V4 pin-hole SANS facility [9] of BENSC in HMI Berlin is presented. The original data evaluation procedure [10] (numerical modeling and fitting) allows - in many cases - to estimate well the volume fraction of the precipitates even without the knowledge on the scattering contrast. The results of the microstructural investigations are related to the used heat treatment procedures.

## 2. Microstructural Model and Data Evaluation

SANS method [11] is based on the measurement of coherently and elastically scattered neutrons to relatively small scattering vector magnitudes  $Q$  ( $Q = |\mathbf{Q}| = |\mathbf{k} - \mathbf{k}_0|$ , where  $\mathbf{k}_0$  and  $\mathbf{k}$  are the wave-vectors of the incident and the scattered neutron, respectively, and  $|\mathbf{k}| = |\mathbf{k}_0| = 2\pi/\lambda$ ,  $\lambda$  denotes the neutron wavelength). The intensity near to the



forward scattering is usually detected by a two-dimensional position-sensitive detector (PSD). The form of the measured macroscopic differential cross-section  $d\Sigma/d\Omega$  in dependence on  $Q$  (or in dependence on components  $Q_x$  and  $Q_y$  in the case of anisotropic scattering) is determined by average microstructural parameters in the irradiated volume (usually  $\sim 50 \text{ mm}^3$ ).

Because of the anisotropic nature of microstructure in the case of single-crystal superalloys, the corresponding scattering pattern is strongly anisotropic (the term anisotropic scattering means here that the azimuthal dependence of scattering on PSD exists). Two-dimensional SANS curves provide information on the average shape of the cuboidal  $\gamma'$ -precipitates [12] (when they are measured in the asymptotic region, i.e. at relatively high  $Q$  values) as well as on the precipitate dimension and distances between them [13] (when the central part of the curve near to the forward scattering is examined). However, standard evaluation methods suited for treatment of isotropic-scattering data cannot be employed here.

In order to interpret the measurements in detail, an appropriate model representing the microstructure had to be selected. Simulations showed that model of perfect cubic particles precisely oriented with edges parallel to  $\langle 100 \rangle$  crystallographic directions does not correspond to the data and an improved model had to be used. At present, a model of cubes or cuboids which are ordered into a three-dimensional grid is employed in the data treatment. The use of many particles in one model ensures, that the interparticle interference is automatically included. The distance between particles becomes one more parameter of the model. The form of one cuboidal particle is a cube having rounded edges. The ratio “radius of curvature of the cuboid edges”/“original-cube edge size” is the only parameter which fully describes the shape of the model [12, 13]. Another feature which can influence the scattering curve is that the precipitates are not perfectly aligned in one direction. This effect is simulated by a spatial orientation distribution of precipitates.

The model is transformed to the reciprocal space by three-dimensional Fast Fourier Transform. After successive corrections to various smearing effects (e.g. multiple scattering corrections, resolution-function smearing), the resulting modeled two-dimensional scattering curve is compared with the measured data. The parameters of microstructure can be refined in an external loop. The detailed description of the procedure can be found in ref. [10, 14].

### 3. Measurements and Results

#### 3.1 ZS26 superalloy

The influence of heat treatment parameters on the final microstructure was studied in ZS26 superalloy [15]. The curves in Fig. 2 correspond to two different morphologies which result from different annealing of the superalloy.

It should be noted, that the size of precipitates (above  $0.5 \mu\text{m}$ ) cannot be directly seen from the measured two-dimensional curves. It is too large for the measured range

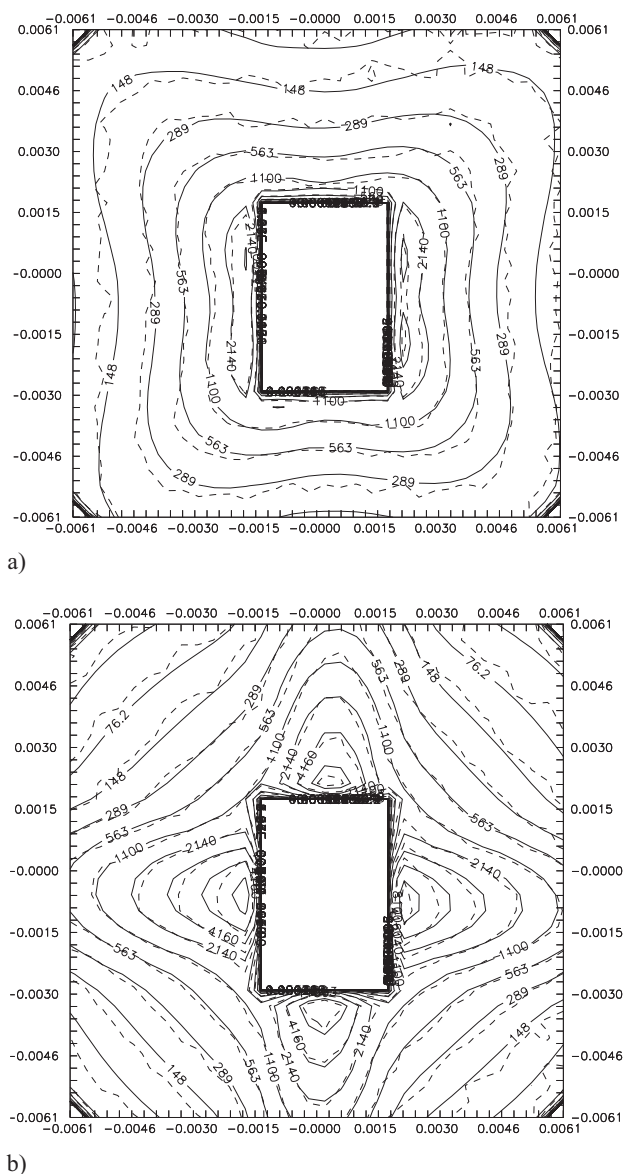


**Fig. 2.** Measured (dashed lines) and fitted (solid lines) two-dimensional curves of two selected ZS26 samples. Heat treatment: (a)  $1280^\circ\text{C}/12\text{h}/\text{N}_2$  (i.e. quenching in liquid nitrogen) +  $1050^\circ\text{C}/16\text{h}/\text{N}_2$  +  $760^\circ\text{C}/16\text{h}/\text{furnace}$ , (b)  $1280^\circ\text{C}/12\text{h}/\text{N}_2$  +  $1160^\circ\text{C}/6\text{h}/\text{N}_2$  +  $840^\circ\text{C}/12\text{h}/\text{furnace}$ ; the crystallographic direction [100] was parallel to the horizontal edge of the PSD in the case b) and tilted by  $45^\circ$  in the case a). The incident beam passed along [001] crystallographic direction in both cases. The description for this and all following two-dimensional scattering curves in the paper: the  $Q$ -ranges on both horizontal and vertical axes are in  $\text{\AA}^{-1}$  and displayed contour lines correspond to the equidistant levels of the macroscopic differential cross-section  $d\Sigma/d\Omega$  (in  $\text{cm}^{-1}\text{sr}^{-1}$ ) in the logarithmic scale.

of scattering vectors to be determined. Only the thickness of the  $\gamma$ -phase layer between  $\gamma'$  precipitates - which is significantly lower - can be extracted. The size of precipitates was calculated with help of complementary double-crystal small-angle neutron scattering which provided center-to-center distance between particles [16]. Afterwards, volume fraction was calculated from the refined geometrical parameters even without knowledge of the scattering contrast, which can be frequently difficult to determine in these alloys [5]. Large precipitates (size about  $1 \mu\text{m}$ ) and large

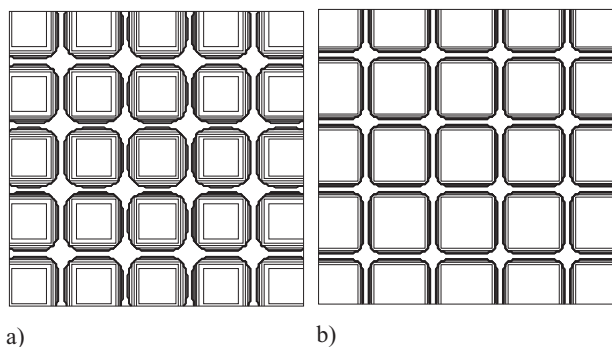


**Fig. 3.** The projections of the real-space models to the PSD plane for two of the measured samples. a), b): heat treatments as well as the corresponding scattering curves can be found in Fig.2a and

volume fractions (approximately 70%) were determined from the measurements for the samples heat treated in three steps.

The projections of the refined real-space models for two of the measured samples are depicted in Fig. 3. The comparison of all the examined specimens revealed that the main influence on the shape is related to the second step of the heat treatment [13].

### 3.2 TCP phase in SC16

As the second example, the interesting feature revealed in SC16 superalloy (composition described elsewhere [17]) is presented. The superalloy was recently developed for applications in land-based gas turbines and it is a subject of the extensive research program in Hahn- Meitner-Institut, Berlin.

In certain low-index orientations of some SC16 samples, additional streaks not belonging to the cuboidal  $\gamma'$ -precipitates were observed. For example, the scattering pattern in Fig. 4a originates from SC16 sample after solution treatment and aging. It contains large  $\gamma'$  precipitates (size around  $0.34 \mu\text{m}$ ) which give rise to the higher scattering intensities along [100] and [010] than in other directions.

However, additional narrow streaks in  $\langle 320 \rangle$  crystallographic directions were detected, too. The effect is more pronounced in the sample which was only water quenched and thus contains only low volume fraction of small (mean size approximately  $250 \text{ \AA}$ ) precipitates (see Fig. 4b). Here the effect of additional scattering particles is obvious [18].

Simulations and additional measurements with different orientations of samples were performed to obtain more information on these additional particles. The experiments showed that the scattering is caused by plate-like particles oriented perpendicular to  $\langle 320 \rangle$  and  $\langle 111 \rangle$  directions for solution treated and aged sample whereas solution treated sample exhibited only particles perpendicular to  $\langle 320 \rangle$  [19]. The scattering was modeled by using oriented disc-like particles having thickness  $> 4000 \text{ \AA}$  and diameter  $> 1 \mu\text{m}$ . From the result of refinement (in combination with other applied experimental methods), the volume fraction of additional particles was estimated to be much less than 1%. Therefore, these particles were not easily observable

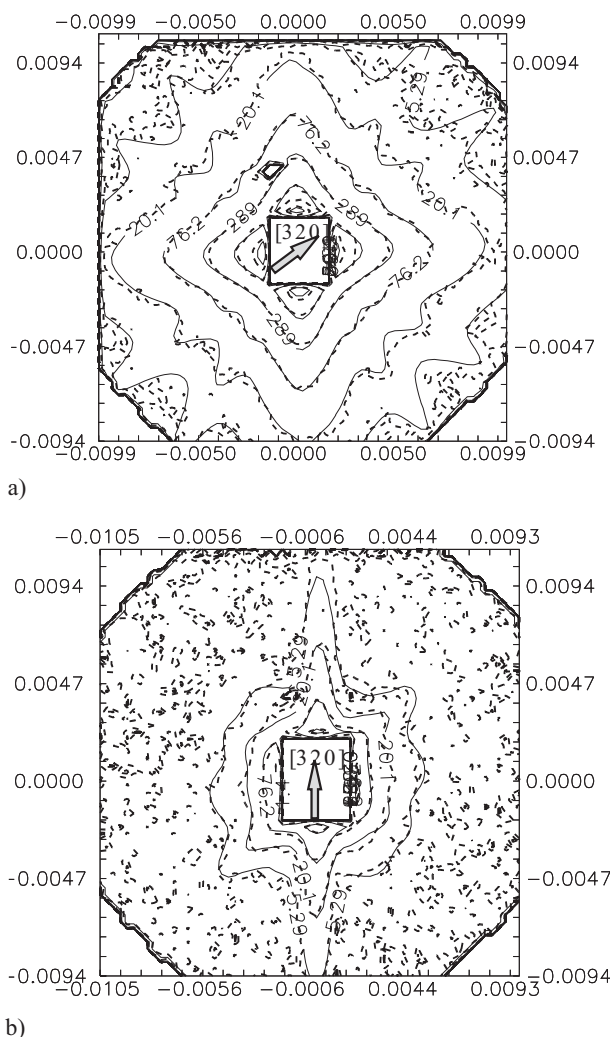


**Fig. 4.** Scattering patterns from a) solution treated and aged sample ( $1350^\circ\text{C}/3\text{h}/\text{WQ} + 1100^\circ\text{C}/1\text{h}/\text{AC} + 850^\circ\text{C}/24\text{h}/\text{AC}$ , where WQ means water quenching and AC air cooling), crystallographic direction [001] parallel to the incident-beam axis, direction [100] parallel to the horizontal edge of the PSD; b) only solution treated sample ( $1350^\circ\text{C}/3\text{h}/\text{WQ}$ ), orientation: crystallographic direction [320] vertical, then rotation around the [320] axis by  $45^\circ$ .

by techniques other than SANS (TEM, SEM, X-ray, light microscopy).

Finally, we arrived at the conclusion that the scattering can be ascribed to precipitates of  $\sigma$ -phase [20] which is one of the topologically close packed (TCP) phases. As far as the authors know, this phase was not yet reported in SC16 after standard heat treatments. For better imagination, Fig. 5 shows TEM micrograph of the plate-like precipitate of  $\sigma$ -phase in another nickel superalloy. TCP phases are detrimental to the mechanical properties because of a scavenging effect of some elements which depletes matrix and because they promote initiation of cracks. Therefore, their detection (even though they occupy only small volume fraction) is desirable.

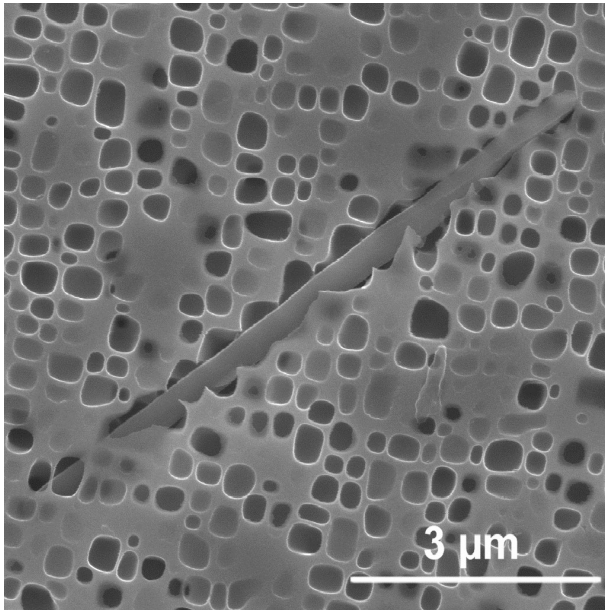


Fig. 5. TEM image of  $\sigma$ -plate in SCA superalloy.

### 3.3. Influence of aging on precipitate morphology in SCA superalloy

The illustration of the recent microstructural investigation of a new superalloy (named SCA) is presented as the last example. An influence of aging on  $\gamma'$ -precipitate microstructure was studied.

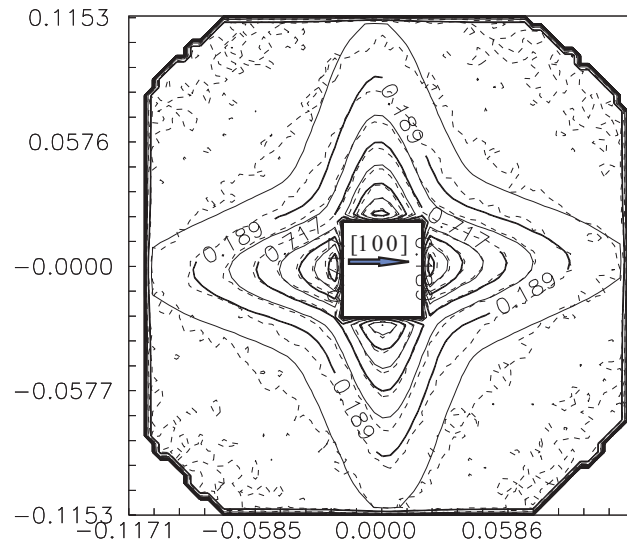
Fig. 6. displays scattering curve from one of measured samples at high and at small scattering vectors. At low  $Q$ -values, the interparticle interference has to be taken into account as can be recognized from the measured interference peaks. The peaks provide information on the average center-to-center distance between neighboring cuboidal precipitates (1970 Å).

The mean size of precipitates was found to be equal to 1540 Å. The spatial orientation distribution of abscissas between centers of precipitates was optimally modeled by a Gaussian function with full width in the half maximum (FWHM) approximately equal to 30°. The geometrical volume fraction was found to be 0.49 and corresponding refined scattering contrast was equal to  $6.2 \cdot 10^9 \text{ cm}^{-2}$ .

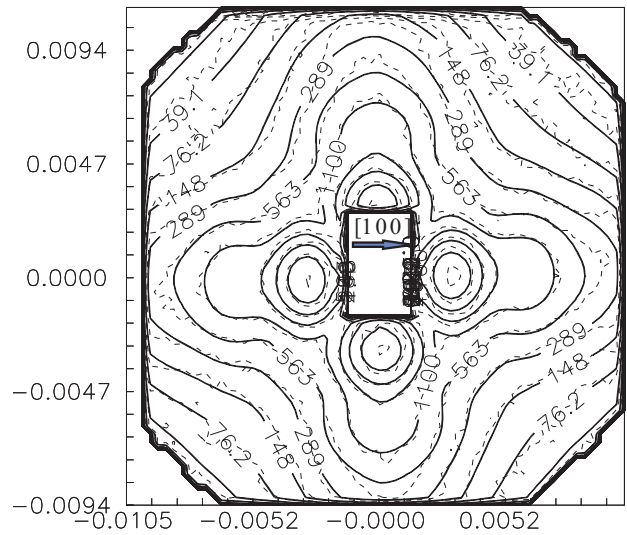
## 4. Conclusions

Small-angle neutron scattering provides useful information on morphology of precipitates (average shape, mean size, distance, orientation distribution) in single-crystal nickel-base superalloys. This method thus contributes substantially to the material research of Ni-base superalloys, i.e. to the understanding of the link between the heat treatment parameters, the microstructural parameters and the mechanical properties.

The determination of volume fraction from the SANS measurement is not necessarily conditional on the knowledge of the scattering contrast. If the geometrical parameters of the microstructure are refined, the volume of scattering particles can be well estimated.



a)



b)

Fig. 6. Scattering curve for SCA sample (heat treatment  $5b^{1/4}$ :  $1285^\circ\text{C}/4\text{h}/\text{AC} + 1100^\circ\text{C}/\frac{1}{4}\text{h}/\text{AC}$ ) at (a) high and (b) small magnitudes of scattering vector. Crystallographic direction [001] was parallel to the incident-beam axis.

In the case of SC16, the SANS experiment revealed the presence of very small volume fraction of well oriented TCP phase which could not be effectively determined and characterized by another experimental method. SANS can detect this phase because of relatively low scattering contrast of  $\gamma'$  precipitates and due to the fact that scattering from precipitates of  $\sigma$ -phase is concentrated along several crystallographic directions only.

In the near future, the authors intend to extend the investigation of SCA superalloy and to test the possibility to study the microstructure of creep exposed samples at V4 facility. The authors also aim to improve the data evaluation procedure, mainly in order to enable a treatment of three-dimensional scan through the reciprocal space in one evaluation cycle.



### Acknowledgement

One of the authors (P. Strunz) was supported by the European Commission through the PECO program "Access to large-scale facilities" during the experiments in HMI Berlin. The same author is grateful to the Grant Agency of the Czech Republic for its financial support for presented work under the contracts 202/97/P041 and 202/97/K038.

### References

1. G. Kostorz, *J. Appl. Cryst.*, **24** (1991) 444-456.
2. G. Kostorz, *Physica Scripta*, **T49** (1993) 636-643.
3. P. Fratzl, F. Langmayr and O. Paris, *J. Appl. Cryst.*, **26** (1993) 820-826.
4. O. Paris, M. Fähmann and P. Fratzl, *Phys. Rev. Lett.*, **75** (1993) 3458-3461.
5. R. Gilles, D. Mukherji, P. Strunz, A. Wiedenmann and R. Wahi, *Z. Metallkd.*, **88** (1997) 518-521.
6. H. A. Calderon, P. W. Voorhees, J. L. Murray and G. Kostorz, *Acta Metall. Mater.*, **42** (1994) 991-1000.
7. A. D. Sequeira, H. A. Calderon, G. Kostorz and J. S. Pedersen, *Acta Metall. Mater.*, **43** (1995) 3427-3439.
8. M. Fähmann, P. Fratzl, O. Paris, E. Fähmann and W. C. Johnson, *Acta Metall. Mater.*, **43** (1995) 1007-1022.
9. U. Keiderling and A. Wiedenmann, *Physica B*, **213&214** (1995) 895.
10. P. Strunz and A. Wiedenmann, *J. Appl. Cryst.*, **30** (1997) 1132-1139.
11. G. Kostorz, In *Neutron Scattering*, ed. G. Kostorz, Academic Press, New York, pp. 227, 1979.
12. P. Strunz, J. Zrník, A. Wiedenmann and P. Lukáš, In *Proc. of EUROMAT 95, Padua/Venice (Italy)*, 25-29.9.1995, pp. 499-502, 1995, Milano: Associazione Italiana di Metallurgia.
13. P. Strunz, A. Wiedenmann, J. Zrník and P. Lukáš, *J. Appl. Cryst.*, **30** (1997) 597-601.
14. P. Strunz, Proceedings of the International School and Symposium on Small-Angle Scattering, Mátraháza, Hungary, October 8-11, 1998, ed. S. Borbély & L. Rosta. KFKI-1999-02/E Report (1999).
15. J. Zrník, M. Hazlinger, M. itňanský and Z. G. Wang, *J. Mater.Sci.Technol.*, **2** (1995) 1-5.
16. P. Strunz, J. Šaroun, P. Mikula, P. Lukáš and F. Eichhorn, *J. Appl. Cryst.*, **30** (1997) 844-848.
17. R. Gilles, D. Mukherji, P. Strunz, A. Wiedenmann and R. P. Wahi, *Physica B*, **234-236** (1997) 1008-1010.
18. R. Gilles, D. Mukherji, P. Strunz, A. Wiedenmann and R. P. Wahi, *Physica B* **241** (1998) 347-349.
19. R. Gilles, D. Mukherji, P. Strunz, B. Barbier, A. Wiedenmann and R. P. Wahi, *Scripta Materialia* **38** (1998) 803-809.
20. C. T. Sims, The occurrence of topologically close packed phases. In *The Superalloys*, eds. C.T. Sims and W. C. Hagel, John Wiley&Sons, New York, USA, pp. 259, 1972.